Article ID: 1007-4627(2016) 03-0274-07

Forward-backward Emission of Target Evaporated Fragments in Nucleus-emulsion Collisions at a few Hundred MeV/nucleon

YANG Ruixia，XU Mingming，MA Tianli，ZHANG Zhi，SHI Rui，ZHANG Donghai

(*Institute of Modern Physics, Shanxi Normal University, Linfen 041004, Shanxi, China*)

Abstract: The multiplicity distribution, multiplicity moment, scaled variance, entropy and reduced entropy of target evaporated fragments emitted in forward and backward hemispheres in 150 AMeV ^{4}He-AgBr, 290 AMeV ^{12}C-AgBr, 400 AMeV ^{12}C-AgBr, 400 AMeV ^{20}Ne-AgBr and 500 AMeV ^{56}Fe-AgBr interactions are investigated. It is found that the multiplicity distribution of target evaporated fragments emitted in both forward and backward hemispheres can be fitted by a Gaussian distribution. The multiplicity moments of target evaporated particles emitted in the forward and backward hemispheres increase with the order of the moment q, and the second-order multiplicity moment is energy independent over the entire energy range for all the interactions in the forward and backward hemisphere. The scaled variance, a direct measure of multiplicity fluctuations, is close to one for all the interactions, which indicate a weak correlation among the target evaporated fragments. The entropy of target evaporated fragments emitted in forward and backward hemispheres are the same respectively for all of the interactions, within experimental errors.

Key words: heavy ion collision; target fragmentation; multiplicity; nuclear emulsion

CLC number: O571.6 **Document code:** A **DOI:** 10.11804/NuclPhysRev.33.03.274

1 Introduction

Target fragments multiplicity is an important variable which can help to test different phenomenological and theoretical models and to understand the mechanism of target fragmentation. In high energy nucleus-emulsion collisions, target fragmentation produces target recoil protons and target evaporated fragments. In emulsion terminology[1], the target recoil protons are referred to as "grey track particles" and the target evaporated fragments are referred to as "black track particles". The grey track particle is formed due to the target recoil protons with the medium energy of $30 \sim 400$ MeV, which is supposed to carry some information about the interaction dynamics because the time scale of the emission of these particles is of the same order ($\approx 10^{-22}$ s) as that of the produced particles. These protons are the low energy part of the internuclear cascade formed in high energy interactions. The black track particles are of low energy (< 30 MeV) single or multiply charged fragments, and they are emitted at the late stage of nuclear reactions and are expected to remember the parts of the history of interactions.

According to the cascade evaporation model[2], the shower particle and the grey track particle are emitted from the nucleus very soon after the instant of impact, leaving the hot residual nucleus in a highly excited state. Indeed, the excitation energy may sometimes be comparable with the total binding energy of the nucleus. Emission of black track particles from this state, however, now takes place relatively slowly. In order to escape from the residual nucleus, a particle must await a favorable statistical fluctuation arising out of random collisions among the nucleons. Emission occurs if, due to a fluctuation, the particle is both close to the nuclear boundary, traveling in an outward direction, and if its kinetic energy is greater than its binding

Received date: 8 Oct. 2015; **Revised date:** 19 Oct. 2015

Foundation item: National Natural Science Foundation of China(11075100); Natural Science Foundation of Shanxi Province (2011011001-2); Shanxi Provincial Foundation for Returned Overseas Chinese Scholars(2011-58)

Biography: YANG Ruixia(1989-), female, Yingxian, Shanxi, postgraduate, working on the field of particle physics and nuclear physics; Email: 404130685@qq.com

Corresponding author: ZHANG Donghai, E-mail: zhangdh@dns.sxnu.edu.cn.

energy. After the evaporation of this particle, a further relatively long period on a nuclear time scale, say 10^{-17} s, will commonly elapse before a second particle is also placed in conditions favorable for escape, and so on. The process continues until the excitation energy of the residual nucleus is so small that transition to the ground state is likely to be effected by the emission of gamma rays. In the rest system of the target nucleus, the emission of evaporated particles is assumed to be isotropic over the whole phase space, and the multiplicity distribution of the evaporated fragments in forward and backward hemispheres should be the same. The evaporation model is based on the assumption that statistical equilibrium has been established in the decaying system and the lifetime is much longer than the time taken to distribute the energy among nucleons within the nucleus. This isotropic emission property may be distorted by the electromagnetic field from the projectile, and other mechanism, such as so called side splash phenomenon[3], may play an important role in the formation of target evaporated fragments and influence the distribution of the particles. In our recent studies[4–5], it has been shown that the angular distribution of black track particles from relativistic nucleus-nucleus interactions are not isotropic, and the averaged multiplicities in the forward hemisphere (emission angle $\theta \leqslant 90°$) are greater than those in the backward hemisphere. These results could not be explained satisfactorily by the evaporation model.

Ghosh *et al.*[6] studied the emission properties of the target evaporated fragments in the forward and backward hemispheres produced in 3.7 *A*GeV ^{12}C-AgBr, 14.5 *A*GeV ^{28}Si-AgBr, 60 *A*GeV ^{16}O-AgBr and 200 *A*GeV ^{32}S-AgBr interactions, and a difference in multiplicity distribution was found in the forward and the backward hemispheres. In our recent paper[5] of the emission properties of the target evaporated fragments in the forward and backward hemispheres produced in 12 *A*GeV ^{4}He-AgBr, 3.7 *A*GeV ^{16}O-AgBr, 60 *A*GeV ^{16}O-AgBr, 1.7 *A*GeV ^{84}Kr-AgBr and 10.7 *A*GeV ^{197}Au-AgBr interactions, the same results as that of Ghosh *et al.*[6] was found. In this paper, the emission properties of the target evaporated fragments in the forward and backward hemispheres produced in 150 *A*MeV ^{4}He-AgBr, 290 *A*MeV ^{12}C-AgBr, 400 *A*MeV ^{12}C-AgBr, 400 *A*MeV ^{20}Ne-AgBr and 500 *A*MeV ^{56}Fe-AgBr interactions are studied. We want to testify if the emission properties of the target evaporated fragments in the forward and backward hemispheres in relativistic energies are still valid or not in intermediate and high energies (a few hundred MeV/nucleon).

2 Experimental details

Five stacks of nuclear emulsion made by Institute of Modern Physics, Shanxi Normal University, were used in present investigation. The emulsion stacks were exposed horizontally at Heavy Ion Medical Accelerator in Chiba (HIMAC), National Institute of Radiological Science (NIRS), Japan. The beams were 150 *A*MeV ^{4}He, 290 *A*MeV ^{12}C, 400 *A*MeV ^{12}C, 400 *A*MeV ^{20}Ne and 500 *A*MeV ^{56}Fe respectively, and the flux was about 3 000 ions/cm^2. BA2000 and XSJ-2 microscopes with a 100× oil immersion objective and 10× ocular lenses were used to scan the plates. The tracks were picked up at a distance of 5 mm from the edge of the plates and were carefully followed until they either interacted with emulsion nuclei or escaped from the plates. Interactions which were within 30 μm from the top or bottom surface of the emulsion plates were not considered for final analysis. All the primary tracks were followed back to ensure that the events chosen do not include interactions from the secondary tracks of other interactions. When they were observed to do so the corresponding events were removed from the sample.

In each interaction all of the secondaries were recorded including shower particle, target recoiled proton, target evaporated fragment and projectile fragments. Shower particles are produced single-charged relativistic particles having velocity $v \geqslant 0.7\ c$, the multiplicity is denoted as $N_{\rm s}$. Grey track particles are mostly the recoiled protons with the kinetic energy of 26 MeV $\leqslant E \leqslant$ 375 MeV and velocity $0.3\ c \leqslant \beta \leqslant 0.7\ c$, the multiplicity is denoted as $N_{\rm g}$. Black track particles are the target evaporated fragments, the multiplicity is denoted as $N_{\rm b}$. Most of the target evaporated fragments are protons with the kinetic energy of $E \leqslant 26$ MeV, little of them are deuteron, tritium, helium, lithium, beryllium and carbon *etc.*, with velocity $\beta \leqslant 0.3\ c$. Grey and black track particles together are called the heavy ionizing particles, the multiplicity is denoted as $N_{\rm h}$. Projectile fragments are the residues of projectile with constant ionization, long range and small emission angle. Details of track classification can be found in our recent paper[7–8].

To ensure that the targets in nuclear emulsion are silver or bromine nuclei, we have chosen only the events with at least eight heavy ionizing track particles ($N_{\rm h} \geqslant 8$).

3 Results and discussion

The general characteristics of 150 *A*MeV ^{4}He-AgBr, 290 *A*MeV ^{12}C-AgBr, 400 *A*MeV ^{12}C-AgBr, 400 *A*MeV ^{20}Ne-AgBr and 500 *A*MeV ^{56}Fe-AgBr inter-

actions, including event statistics($N_{\rm ev}$), average multiplicity of the target evaporated fragments emitted in forward hemisphere ($< n_{\rm b}^{\rm f} >$), backward hemisphere ($< n_{\rm b}^{\rm b} >$) and whole space ($< n_{\rm b} >$), are presented in Table 1. It is found that the proportion of target evaporated fragments emitted in the forward hemisphere is greater than that in the backward hemisphere.

Table 1 Average multiplicity of target evaporated fragments in the forward and backward hemispheres for different nucleus-AgBr interactions.

Beams	$N_{\rm ev}$	$< n_{\rm b}^{\rm f} >$	$< n_{\rm b}^{\rm b} >$	$< n_{\rm b} >$
150 *A*MeV ^{4}He	49	4.33±0.36	2.49±0.25	6.82±0.47
290 *A*MeV ^{12}C	432	5.36±0.13	2.35±0.07	7.88±0.16
400 *A*MeV ^{12}C	250	6.40±0.21	3.12±0.12	9.52±0.28
400 *A*MeV ^{20}Ne	277	5.13±0.16	2.63±0.09	7.76±0.20
500 *A*MeV ^{56}Fe	558	5.33±0.15	2.20±0.07	7.53±0.19

Figs. 1 to 5 show the multiplicity distributions of target evaporated fragments emitted in the forward hemisphere, backward hemisphere and the whole space. It is found that the distributions can be well fitted by a Gaussian distribution for 150 *A*MeV ^{4}He-AgBr, 290 *A*MeV ^{12}C-AgBr, 400 *A*MeV ^{12}C-AgBr, 400 *A*MeV ^{20}Ne-AgBr and 500 *A*MeV ^{56}Fe-AgBr interaction. The Gaussian fitting parameters (mean value and error) and χ^2/DOF are presented in Table 2, where DOF means the degree of freedom of simulation. It is found that the fitting parameters are different between the forward and backward hemispheres for all the interactions, and the mean values and errors of Gaussian distributions in the forward hemisphere are greater than that in the backward hemisphere. The difference in the nature of multiplicity distributions between the two hemispheres may be attributed to the fact that the mechanism of the target fragmentation process is different in the forward and backward hemispheres. Based on the cascade evaporation model[2], the emission of the target evaporated fragments should be isotropic in the laboratory frame, but due to the electromagnetic field from the projectile, the emission of target evaporated fragments is close to $\theta_{\rm Lab} \approx 90^{\circ}$ symmetric and the emission probability in the forward hemisphere is greater than that in the backward hemisphere. According to the model proposed by Stocker *et al.*[3], the emission of target fragments in the backward hemisphere can be explained with the help of the side splash phenomenon. In a nucleus-nucleus collision, a head shock zone may be developed during the dividing phase of the projectile nucleus with the target. A strongly compressed and highly excited projectile-like object continues to interpenetrate the target with supersonic velocity and may push the matter sideways. This results in the generation of shock waves that give rise to particle evaporation in the backward directions. At intermediate impact parameters the highly inelastic bounce-off appears, where the large compression pot-

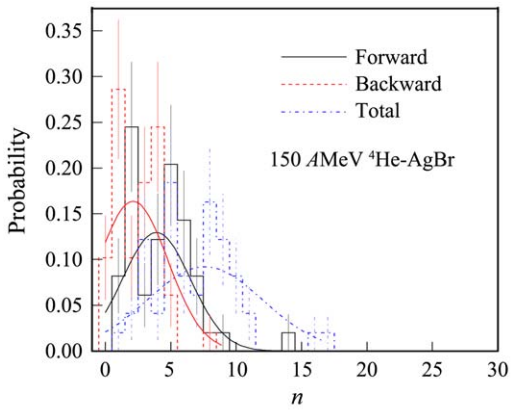

Fig. 1 (color online) Multiplicity distributions of target evaporated fragments emitted in 150 *A*MeV ^{4}He-AgBr interactions, the smooth curves are the results from the Gaussian fitting.

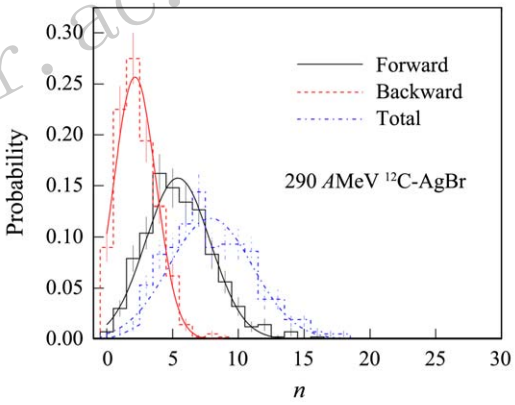

Fig. 2 (color online) Multiplicity distributions of target evaporated fragments emitted in 290 *A*MeV ^{12}C-AgBr interactions, the smooth curves are the results from the Gaussian fitting.

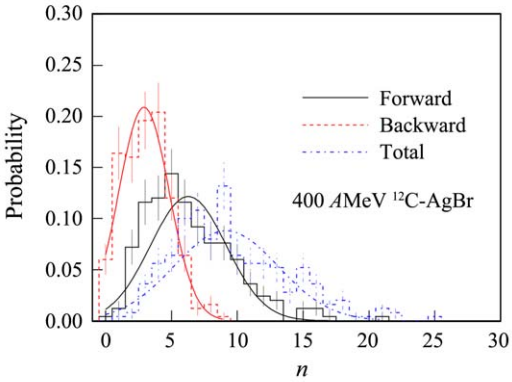

Fig. 3 (color online) Multiplicity distributions of target evaporated fragments emitted in 400 *A*MeV ^{12}C-AgBr interactions, the smooth curves are the results from the Gaussian fitting.

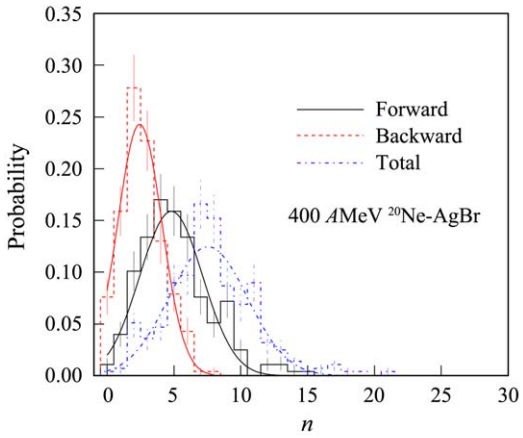

Fig. 4 (color online) Multiplicity distributions of target evaporated fragments emitted in 400 *A*MeV ^{20}Ne-AgBr interactions, the smooth curves are the results from the Gaussian fitting.

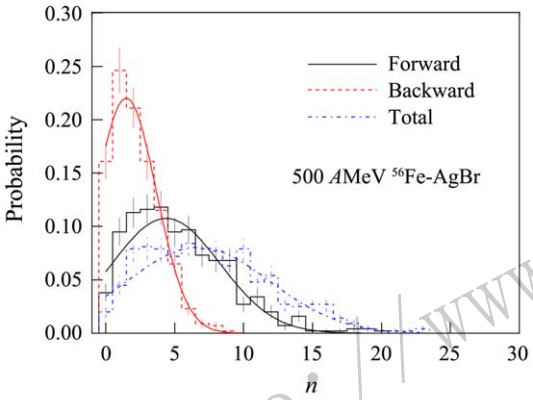

Fig. 5 (color online) Multiplicity distributions of target evaporated fragments emitted in 500 *A*MeV ^{20}Fe-AgBr interactions, the smooth curves are the results from the Gaussian fitting.

ential leads to the sideways deflection of the projectile, which then explodes. A large collective transverse momentum transfer to the target leads to azimuthally asymmetric fragment distribution.

The multiplicity distribution also can be studied using the moments of the distribution, which are given by

$$C_q = \frac{< n^q >}{< n >^q} = \frac{\sum_n n^q P_n}{(\sum_n n P_n)^q} \ , \tag{1}$$

where q is a positive integer called the order of the moment and P_n is the probability of producing or emitting n particles. Here

$$< n^q > = \sum_n n^q \frac{\sigma_n}{\sigma_{\rm inel}} \ , \tag{2}$$

where σ_n is the partial cross section for producing or emitting a state of multiplicity n, $\sigma_{\rm inel}$ is the total inelastic cross-section and $< n >$ is the average multiplicity.

The multiplicity moments, sometimes called the reduced C moments, can be used to describe the properties of multiplicity distributions, *e.g.* as a function of the projectile energy. In practice, only the first few moments can be calculated with reasonable accuracy, due to the limited statistics. Table 3 presents the multiplicity moments of target evaporated fragments emitted in the forward and backward hemispheres for 150 *A*MeV ^{4}He-AgBr, 290 *A*MeV ^{12}C-AgBr, 400 *A*MeV ^{12}C-AgBr, 400 *A*MeV ^{20}Ne-AgBr and 500 *A*MeV ^{56}Fe-AgBr interactions, with the corresponding results in Ref. [5] also included. It should be mentioned that the statistical errors of the reduced C moments are greater for 150 *A*MeV ^{4}He-AgBr interaction because of the poor event statistics. This situation is also presented in the results of Table 2. In both the hemispheres, for all the interactions, the multiplicity moments increase with the order of the moment q, and the second order multiplicity moments are energy independent over the entire energy range in the forward and backward hemispheres. In the backward hemisphere, multiplicity moments up to the third order are also energy independent for all the interaction. These results are the same as our recent observation[5] in relativistic energies. The energy-independent behavior of multiplicity moments may hint at the existence of KNO scaling, which is an energy independent scaling law of multiplicity distribution proposed by Koba *et al.*[9].

Table 2 Gaussian fitting parameters of target evaporated fragment multiplicity distributions in the forward and backward hemispheres for different type of nucleus-AgBr interactions.

Beams	Forward hemisphere			Backward hemisphere			Whole space		
	Mean value	Error	χ^2	Mean value	Error	χ^2	Mean value	Error	χ^2
150 *A*MeV ^{4}He	3.908±0.916	2.603±0.762	1.699	2.127±0.771	2.659±0.832	2.232	7.615±1.037	4.410±1.149	0.991
290 *A*MeV ^{12}C	5.411±0.127	2.462±0.097	1.219	2.148±0.088	1.593±0.074	1.281	7.906±0.182	3.164±0.126	1.835
400 *A*MeV ^{12}C	6.287±0.269	2.877±0.201	2.177	2.921±0.145	1.908±0.117	1.191	9.139±0.336	3.592±0.273	1.828
400 *A*MeV ^{20}Ne	4.803±0.191	2.354±0.180	1.923	2.445±0.115	1.662±0.106	1.070	7.559±0.190	2.939±0.162	1.379
500 *A*MeV ^{56}Fe	4.376±0.230	3.915±0.210	1.724	1.484±0.185	2.185±0.135	0.794	6.712±0.282	5.167±0.269	1.277

Table 3 Values of the multiplicity moments of target evaporated fragment multiplicity distributions in the forward and backward hemispheres for different type of nucleus-AgBr interactions.

Beams	Forward hemisphere			Backward hemisphere			Reference
	C_2	C_3	C_4	C_2	C_3	C_4	
150 *A*MeV ^{4}He	1.324±0.453	2.188±1.248	4.425±1.972	1.468±0.544	2.581±1.481	5.240±2.954	Present
290 *A*MeV ^{12}C	1.223±0.110	1.732±0.241	2.766±0.295	1.418±0.171	2.447±0.465	4.953±0.938	Present
400 *A*MeV ^{12}C	1.279±0.174	1.980±0.425	3.576±0.506	1.343±0.187	2.102±0.437	3.687±0.707	Present
400 *A*MeV ^{20}Ne	1.268±0.158	1.914±0.369	3.320±0.478	1.354±0.183	2.160±0.437	3.889±0.749	Present
500 *A*MeV ^{56}Fe	1.460±0.164	2.667±0.466	5.745±0.702	1.612±0.201	3.224±0.609	7.517±1.430	Present
12 *A*GeV ^{4}He	1.38±0.06	2.35±0.17	4.67±0.24	1.41±0.06	2.43±0.17	4.87±0.29	[5]
3.7 *A*GeV ^{16}O	1.28±0.09	1.94±0.21	3.35±0.25	1.31±0.09	2.02±0.22	3.52±0.32	[5]
60 *A*GeV ^{16}O	1.22±0.10	1.74±0.23	2.87±0.25	1.23±0.10	1.72±0.21	2.65±0.26	[5]
1.7 *A*GeV ^{84}Kr	1.24±0.16	1.77±0.34	2.84±0.40	1.33±0.22	2.30±0.60	4.66±0.84	[5]
10.7 *A*GeV ^{197}Au	1.29±0.11	1.94±0.24	3.25±0.34	1.39±0.13	2.32±0.35	4.50±0.60	[5]

It is known that the probability of multiplicity can be used to evaluate the entropy of the produced particles. The entropy of the produced particles can be calculated using the formula defined by Wehrl[10] as

$$S = -\sum_n P_n \ln P_n \ . \tag{3}$$

Here P_n is the probability of having n produced particles in the final state such that $\sum P_n = 1$ for any phase space interval. The parameter entropy is related to the fractal dimension, to be more specific, the information dimension[11–12]. The entropy is invariant under an arbitrary distortion of multiplicity scale; in particular, if a sub-sample of particles, such as charged particles, is chosen. Using Eq. (3), we have calculated the entropy and the reduced entropy ($S/ < n >$), *i.e.* the ratio of the entropy to average multiplicity of target evaporated fragments in the forward and backward hemisphere for all the nucleus-nucleus interactions we have investigated. Table 4 presents our results together with the corresponding results in Ref. [5]. It is found that the entropy value of the target evaporated fragments emitted in the forward hemisphere is greater than that emitted in the backward hemisphere, and the values of entropy remain almost energy independent in both hemispheres.

Table 4 Values of entropy, reduced entropy and scaled variance of target evaporated fragments in the forward and backward hemispheres for different type of nucleus-AgBr interactions.

Beams	Forward hemisphere			Backward hemisphere			Reference
	S	$S/<n>$	w	S	$S/<n>$	w	
150 *A*MeV ^{4}He	2.022±0.536	0.467±0.130	1.400±0.196	1.730±0.330	0.695±0.149	1.166±0.024	Present
290 *A*MeV ^{12}C	2.338±0.285	0.422±0.052	1.235±0.020	1.777±0.148	0.757±0.067	0.980±0.017	Present
400 *A*MeV ^{12}C	2.516±0.440	0.393±0.070	1.787±0.077	1.974±0.224	0.633±0.070	1.070±0.000	Present
400 *A*MeV ^{20}Ne	2.308±0.339	0.451±0.068	1.376±0.041	1.823±0.178	0.694±0.072	0.930±0.005	Present
500 *A*MeV ^{56}Fe	2.593±0.327	0.486±0.063	2.450±0.052	1.857±0.138	0.843±0.069	1.353±0.016	Present
12 *A*GeV ^{4}He	2.38±0.12	0.52±0.03	1.76±0.02	2.20±0.09	0.60±0.03	1.50±0.01	[5]
3.7 *A*GeV ^{16}O	2.54±0.25	0.42±0.04	1.72±0.02	2.29±0.18	0.51±0.04	1.39±0.01	[5]
60 *A*GeV ^{16}O	2.36±0.27	0.39±0.05	1.32±0.04	2.28±0.23	0.45±0.04	1.15±0.01	[5]
1.7 *A*GeV ^{84}Kr	2.49±0.44	0.39±0.07	1.51±0.02	2.26±0.37	0.54±0.08	1.52±0.07	[5]
10.7 *A*GeV ^{197}Au	2.38±0.23	0.47±0.05	1.46±0.01	2.17±0.20	0.60±0.06	1.41±0.02	[5]

Finally, we want to evaluate the multiplicity correlation among the target evaporated fragments in the forward and backward hemispheres respectively. A useful measure of the fluctuation of any variable is the ratio of its variance to its mean value, so the variance of the multiplicity distribution can be used to measure the multiplicity fluctuations. In order to study the multiplicity fluctuations in high energy nucleus-nucleus collisions, we use a scaled variable w suggested by Ghosh *et al.*[6] such that

$$w = \frac{< n^2 > - < n >^2}{< n >} \ . \tag{4}$$

A direct measure of the scaled variance would give a direct measure of multiplicity fluctuation. Multiplicity fluctuation is but one aspect of a two-particle correlation function. The study of the scaled variance can very easily reveal the nature of correlation among the produced particles. If the value of w is much greater than 1, it may be said that there is a strong correlation among the produced particles. In contrast, if the value

of w is close to one, weak correlation is indicated.

The values of the scaled variance w for all of the interactions were calculated in order to quantify the correlations among the target evaporated fragments emitted in forward and backward hemispheres for 150 AMeV ^{4}He-AgBr, 290 AMeV ^{12}C-AgBr, 400 AMeV ^{12}C-AgBr, 400 AMeV ^{20}Ne-AgBr and 500 AMeV ^{56}Fe-AgBr interactions. The result of the scaled variance is also presented in Table 4. It is found that the values of the scaled variance in backward hemisphere are much close to 1 for all of the interactions, and the value of scaled variance in the forward hemisphere is greater than that in the backward hemisphere for each interaction. In both forward and backward hemisphere the scaled variances are close to one, which suggested that there is a weak correlation in production of the target evaporated fragments. Comparing these results with ones[5] obtained in relativistic energies, it can conclude that the target fragmentation is independent of the projectile energy.

4 Conclusions

The multiplicity distribution, multiplicity moment, scaled variance, entropy and reduced entropy of target evaporated fragment emitted in forward and backward hemispheres in 150 AMeV ^{4}He-AgBr, 290 AMeV ^{12}C-AgBr, 400 AMeV ^{12}C-AgBr, 400 AMeV ^{20}Ne-AgBr and 500 AMeV ^{56}Fe-AgBr interactions have been investigated. It is found that the multiplicity distribution of target evaporated fragments emitted in forward and backward hemispheres can be fitted by a Gaussian distribution. The Gaussian fitting parameters are different between the forward and backward hemispheres for all the interactions, which may indicate that the nature of the emission of target evaporated particles differs between the two hemispheres. The multiplicity moments of target evaporated particles emitted in the forward and backward hemispheres increase with the order of the moment q, and the second-order multiplicity moments of the target evaporated fragments in both hemispheres are energy independent over the entire energy range for all the interactions. The scaled variance, a direct measure of multiplicity fluctuations, is close to one for all the interactions, which may show that there is a weak correlation among the target evaporated fragments. The entropy of target evaporated fragments emitted in the forward and backward hemispheres are the same within experimental errors for all of the interactions, respectively. All of these conclusions are the same as the results obtained in relativistic energies, so the target fragmentation is independent of the projectile energies.

References:

[1] POWELL C F, FOWLER P H, PERKINS D H. The Study of Elementary Particles by the Photographic Method[M]. Pergamon, Oxford, 1959: 432.

[2] POWELL C F, FOWLER P H, PERKINS D H. The Study of Elementary Particles by the Photographic Method[M]. Pergamon, Oxford, 1959: 450.

[3] STOCKER H, MARUHN J A, GREINER W. Z Phys A, 1979, **293**: 173.

[4] ZHANG Donghai, NIU Yaojie, WANG Lichun, *et al*. Chin Phys B, 2010, **19**: 072501.

[5] ZHANG Zhi, MA Tianli, ZHANG Donghai. Chin Phys C, 2015, **39**: 104002.

[6] GHOSH D, DEB A, BHATTACHARYYA S. Phys Scr, 2011, **84**: 015201.

[7] ZHANG Donghai, CHEN Yanling, WANG Guorong, *et al*. Chin Phys C, 2015, **39**: 014001.

[8] ZHANG Donghai, CHEN Yanling, WANG Guorong, *et al*. Nucl Phys Rev, 2014, **31**(2): 126. (in Chinese)
(张东海，陈艳玲，王国蓉，等. 原子核物理评论，2014，**31**(2): 126.)

[9] KOBA Z, NIELSEN H B, OLESEN P. Nucl Phys B, 1972, **40**: 317.

[10] WEHRL A. Rev Mod Phys, 1978, **50**: 221.

[11] SIMAK V, SUMBERA M, ZBOROVSKI I. Phys Lett B, 1988, **206**: 159.

[12] GHOSH D, ROY J, SENGUPTA A G, *et al*. Can J Phys, 1992, **70**: 667.

几百兆电子伏特/核子能区原子核诱发乳胶核反应靶核蒸发碎片前后发射研究

杨瑞霞，徐明明，马田丽，张 智，石 瑞，张东海

(山西师范大学现代物理研究所，山西 临汾 041004)

摘要： 对 150 AMeV ^{4}He-AgBr, 290 AMeV ^{12}C-AgBr, 400 AMeV ^{12}C-AgBr, 400 AMeV ^{20}Ne-AgBr 及 500 AMeV ^{56}Fe-AgBr 作用靶核蒸发碎片在反应前后半球内的多重数分布、多重数矩、标度方差、熵及约化熵分别进行了分析。实验结果表明，靶核蒸发碎片在前后半球内的多重数分布可以用高斯分布来描述。在前后半球内的多重数分布矩分别随秩数的增加而增加，且前后半球内多重数分布二阶矩与反应类型及束流能量无关。对于所有研究的核反应，其标度方差 (一个直接描述多重数涨落的变量) 值接近于 1，表明在前后半球内靶核蒸发的发射存在较弱的关联。在前后半球内靶核蒸发碎片发射过程中的熵及约化熵在实验误差范围内与反应系统无关。

关键词： 重离子碰撞；靶核碎裂；多重数；原子核乳胶

收稿日期： 2015-10-08； **修改日期：** 2015-10-19

基金项目： 国家自然科学基金资助项目(11075100)；山西省自然科学基金资助项目(2011011001-2)；山西省留学归国人员基金资助项目(2011-058)

通信作者： 张东海，E-mail: zhangdh@dns.sxnu.edu.cn。